第 28 卷第 7 期 无 机 化 学 学 报 Vol.28 No.7
2012 年 7 月 CHINESE JOURNAL OF INORGANIC CHEMISTRY 1513-1519

二硫化钼中空微球的制备、表征以及光催化性能

杨依萍 李卓民 杨玉超 邓文礼*
(华南理工大学材料科学与工程学院,广州 510640)

摘要: 以四丁基溴化铵为添加剂,采用水热法制备出直径为 2~5 μm 的二硫化钼(MoS_2)空心微球,研究了反应温度、添加剂量和时间对 MoS_2 物相和形貌的影响。XRD、SEM、EDS、TEM、XPS 表征结果表明, 当反应温度为 240 ℃时可得到结晶良好的六方相 2H-MoS_2,MoS_2 的形貌主要受四丁基溴化铵用量的影响, 随着用量的增多 MoS_2 历经了球状–花球状–不规则堆积状的递变。对 MoS_2 中空微球的形成机制进行了探讨,认为在反应中四丁基溴化铵起到了模板的作用。通过制备样品对罗丹明 B 的降解评估了二硫化钼中空微球的光催化性能,其对罗丹明的降解效率达到 90%。

关键词: 二硫化钼; 微米空心结构; 水热法; 罗丹明 B; 光催化
中图分类号: O614.61+2 **文献标识码**: A **文章编号**: 1001-4861(2012)07-1513-07

Fabrication, Microstructure and Catalytic Degradation Performance of MoS_2 Hollow Microspheres

YANG Yi-Ping LI Zhuo-Min YANG Yu-Chao DENG Wen-Li*
(*College of Materials Science and Engineering, South China University of Technology, Guangzhou* 510640, *China*)

Abstract: Molybdenum disulfide (MoS_2) hollow microspheres with the diameter of 2~5 μm were synthesized using tetrabutylammonium bromide (Bu_4NBr) as an additive by a hydrothermal method. The effect of temperature, time and concentration of Bu_4NBr on the phase and morphology of MoS_2 was investigated. The as-prepared MoS_2 was characterized by X-ray diffraction (XRD), scanning electron microscope (SEM), energy dispersive spectroscopy (EDS), transmission electron microscope (TEM), and X-ray photoelectron spectra (XPS). The results indicate that hexagonal 2H-MoS_2 can be formed at 240 ℃ with good crystallinity. The morphology of MoS_2 crystal is greatly affected by the dosage of Bu_4NBr. With the increase in the concentration of Bu_4NBr, the morphology of MoS_2 changes from microspheres, via ball-flowers, to irregular packing. The templating mechanism is proposed to explain the formation of MoS_2 hollow structures. Photocatalytic results show that the degradation rate of rhodamine B can reach to 90% by the MoS_2 hollow microspheres under visible light irradiation.

Key words: MoS_2; hollow microspheres; hydrothermal synthesis; rhodamine B; photocatalytic activity

Transition metal sulfides have received much attention due to their interesting properties including superconductiveity [1], electrical properties [2], fluorescence[3], and magnetism[4]. As a compound with unique layered structure, MoS_2 has been the subject of much attention for its important applications in solid lubricants[5], potential hydrogen storage[6], field emission tips [7], and solid-state secondary lithium battery cathodes[8]. Considerable efforts have been devoted to the preparation of MoS_2 nano/micromaterials

收稿日期:2011-09-09。收修改稿日期:2012-03-14。
国家自然科学基金(No.51073059,91023002),国家重大研究计划子课题(No.2009CB930604),广东省省部产学科研课题(No.2010B090400123)资助项目。
*通讯联系人。E-mail:wldeng@scut.edu.cn, Tel:+86-020-22236708, Fax: +86-020-22236706; 会员登记号:S060812753M。

with various morphologies, such as fullerene-like structures [9], nanotubes [10], nanorods [11], nanowires and nanoribbons [12], amorphous nanospheres [13], nanoflowers [14], interlayer composite structure [15] and hierarchical hollow cubic cages [16] through techniques including electrochemical/chemical method, hydrothermal method, sonochemical method, gas-solid reaction, chemical vapor deposition (CVD) and ultrasonic spray pyrolysis. Ma et al [17-18] utilized hydrothermal method to prepare MoS_2 microspheres by using sodium silicate or ionic liquid as an additive. Huangs group [19] prepared MoS_2 microspheres by introducing tungsten acid. Hollow MoS_2 microspheres were synthesized by redox reaction in ionic liquids/water binary emulsions [20]. MoS_2 nanospheres with an average diameter of 100 nm were fabricated by surfactant-assisted route[21].

Herein, we present a facile and effective route to synthesize MoS_2 hollow microspheres by employing Bu_4NBr as an additive. The effect of the temperature and additive on the morphology of the products was studied. In addition, the MoS_2 hollow microspheres had photocatalytic activities for degradation of rhodamine B (RhB) under the visible light irradiation.

1 Experimental

1.1 Synthesis of MoS_2 hollow microspheres

All the reagents used were analytical grade and used as received. In a typical procedure, 3.0 mmol of Na_2MoO_4, 9.0 mmol KSCN and 0.9 mmol Bu_4NBr were dissolved in 50 mL distilled water under continuous stirring. Then 10 mol·L^{-1} HCl was dropped into the solution to adjust the pH value to less than 1. After 10 min, the mixture was transferred into a stainless Telfon-lined autoclave. The autoclave was maintained at 160, 200 and 240 ℃, respectively, for 24 h, and then cooled down to room temperature naturally. The dark solid products were filtered, rinsed with distilled water and absolute ethanol three times. Finally the products were dried in vacuum at 60 ℃ for 24 h.

1.2 Characterization

The XRD measurement was performed on a D8 Advance Bruker-AXS diffractometer using Cu $K\alpha$ radiation (λ=0.154 18 nm) operating at 50 kV. The scan rate of 0.02°·s^{-1} was applied to record the pattern in the 2θ range of 10° ~70° . Scanning electron microscope (SEM) images were obtained by a JEOL JSM-7001F field emission scanning electron microscope (FESEM) operated at an accelerating voltage of 10 kV. Transmission electron microscopy (TEM) investigation was carried out using a Japanese JEM-100CX II transmission electron microscopy. X-ray photoelectron spectra (XPS) were examined on an ESCALab MK II X-ray photoelectron spectrometer, using non-monchromatized Mg $K\alpha$ X-ray as excitation source.

1.3 Photocatalytic performance

The photocatalytic activity of the selected MoS_2 sample (Fig.2c) was evaluated according to the decoloration rate of rhodamine B solution in a quartz glass flask. A 250 W sodium lamp was selected as the visible light source. A typical catalytic experiment is described as follows: 0.2 g MoS_2 was added into a 100 mL of rhodamine B solution (20 mg·L^{-1}), and the suspension was put into a dark room by stirring for 10 min. Then the catalytic reaction continued for 90 min under visible light. The light intensity was calculated to be 0.6 mW·cm^{-2}. About 5 mL reaction suspension was sampled by an injector at the time of 0, 5, 15, 30, 45, 60, 75, 90 min, and then was clarified by centrifugation at 3 000 r·min^{-1} for 5 min. The absorbance was measured using a 765 spectrophotometer (Shanghai Precision & Scientific Instrument Company, China). The decoloration rate was accounted for according to the formula: $(A_0-A_i)/A_0$. (A_i represents the absorbance (550 nm) of the obtained solution at the time of i min).

2 Results and discussion

2.1 Structure characterization

The crystal structure and phase purity of the samples were characterized by XRD. Fig.1 shows the XRD patterns of the MoS_2 products synthesized at different temperatures. Fig.1a shows only a broad weak peak beginning at 2θ =30° . The two maxima approximately locate at the (100) and (110) positions for bulk 2H-MoS_2 [22]. The above results indicate that the MoS_2 products obtained at 160 ℃ are amorphous with

poor crystals, which is consistent with that of the earlier work[23]. When the temperature arrives at 200 ℃ (Fig.1b), a new peak is found at 2θ=14.4° (marked by the dotted line in the graph), corresponding to the diffraction from the (002) plane of crystalline MoS_2. However, the (002) peak is rather weak, which suggests that only a few layers of MoS_2 stack along this direction. As shown in Fig.1c, the peaks are much more intensive, which indicates that the crystals of MoS_2 products are much thicker. All the reflections can be readily indexed as hexagonal 2H-MoS_2 [space group $P6_3/mmc$ (194)] with lattice constants a= 0.316 16 nm and c =1.22985 nm, identical to the reported data in the PDF cards (37-1492).

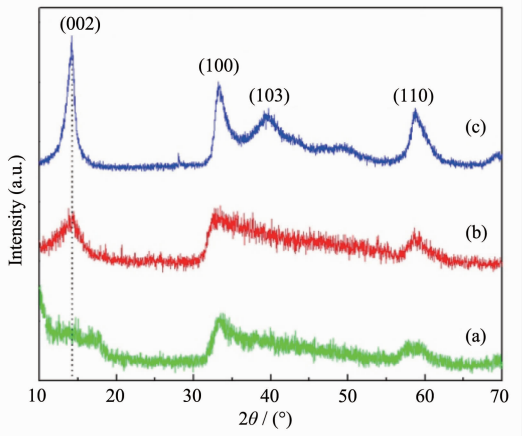

(a) 160 ℃; (b) 200 ℃; (c) 240 ℃

图 1　不同温度下制备的二硫化钼样品的 XRD 图

Fig.1　XRD patterns of MoS_2 samples prepared at different temperatures

2.2　Morphology characterization

Fig.2a shows the SEM image of the irregular MoS_2 microparticles under 160 ℃ with the diameter of several micrometers. However, the particles are clustered together and the gaps between the particles could hardly be observed. When the temperature was up to 200 ℃, sphere-like MoS_2 with irregular morphologies and different sizes (Fig.2b) was prepared. Fig.2c shows that the obtained samples are microspheres with the mean diameter of 4 μm. A high-magnification SEM image (Fig.2c) shows some typical hollow spheres, indicating that the spheres are hollowed, and the thickness of the hollow-sphere shell is 400 ~500 nm. The above results show that the hollow microspheres of MoS_2 could be obtained at the high temperature of 240 ℃. The composition of MoS_2 samples prepared by Bu_4NBr assisted hydrothermal process was analyzed by EDS. The repetitive EDS analysis demonstrates that the samples are composed of Mo and S with the atomic ratio 1:1.9~2.1, which is very close to the theoretical value. This result further confirms that the products are MoS_2. The structural characterization of the MoS_2 microspheres obtained at 240 ℃ was further examined by TEM. Fig.3 exhibits two spheres, which further proves the hollow structures of the as-prepared MoS_2. Further evidence for the quality and composition was obtained by the XPS spectrum for the products. The binding energies obtained in the XPS analysis were corrected for specimen charging by referencing the C1s to 284.6 eV. In Fig.4a, there are two strong peaks at 229.5 eV and 232.6 eV, which are attributed to Mo3$d_{5/2}$ and Mo3$d_{3/2}$[24], respectively. The peaks at 162.3 eV and 169.1 eV (fig.4b) can be indexed to S2$p_{3/2}$ and S2$p_{1/2}$. No obvious peaks are found for other unreacted oxides.

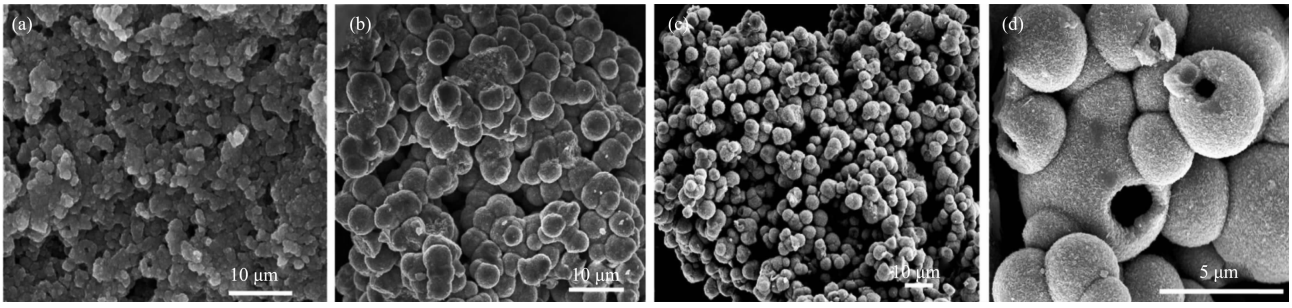

(a) 160 ℃, (b) 200 ℃, (c, d) 240 ℃

图 2　不同温度下添加 0.9mmol Bu_4NBr 制备的 MoS_2 扫描电镜图

Fig.2　SEM images of MoS_2 nanostructures obtained at different temperatures with 0.9 mmol Bu_4NBr

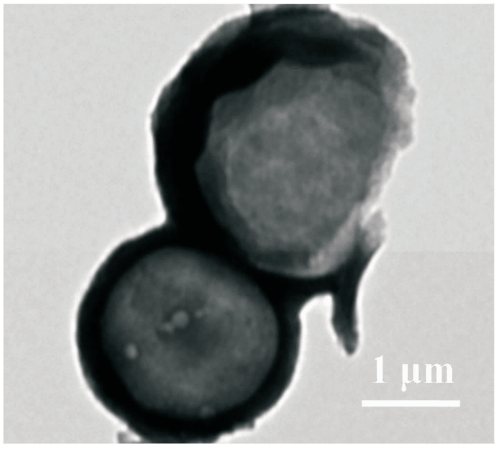

图 3 240 ℃下 MoS_2 的透射电镜图

Fig.3 TEM image of the MoS_2 obtained at 240 ℃

2.3 Effect of reaction parameters

According to the results above, the reaction temperature plays an important role in the formation of morphology and crystallinity of the MoS_2 products. In order to clarify the formation mechanism of MoS_2, we change the amount of Bu_4NBr at 240 ℃, while other conditions are kept constant. As shown in Fig.5a, only rag-like products are obtained when no Bu_4NBr is added. The MoS_2 with rag-like morphology is made of nano-sheets with the diameter of several nanometers (inset of Fig.5a, 500×500 nm). This can be explained by the facts that with the absence of Bu_4NBr, no vessels are formed in the reaction process. When the concentration of Bu_4NBr increases to 0.9 mmol, hollow microspheres are formed (Fig.5b). As 1.5 mmol Bu_4NBr is added, ball-flowers are formed with a diameter of 3~5 μm (Fig. 5c). When Bu_4NBr with much higher concentration (3.0 mmol) is added, the globular MoS_2 begins to reunite into irregular packing (Fig.5d). These results indicate that the additive of Bu_4NBr has a remarkable impact on the morphologies of the final products. Fig.6a~c show the SEM images of MoS_2 prepared at 240 ℃ with 0.9 mmol Bu_4NBr for 16, 24 and 48 h. When the duration increases from 16 h to 48 h, the morphologies do not change much, the diameter of MoS_2 is found to be in the range of 2~6 μm.

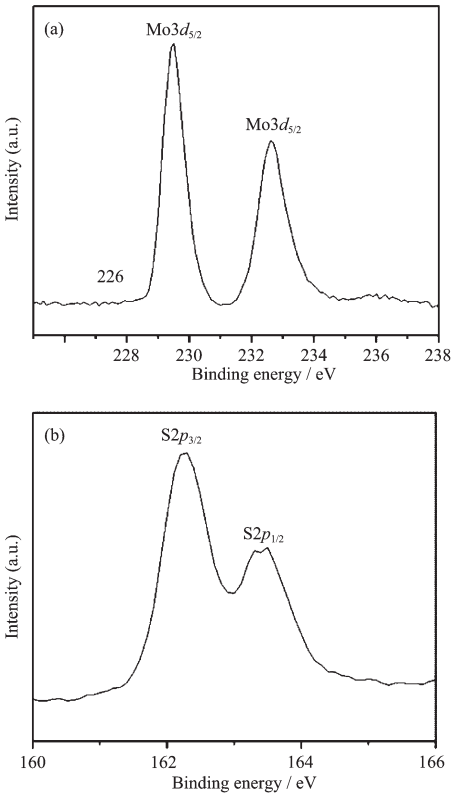

(a) Mo3*d*; (b) S2*p* core-level spectra

图 4 240 ℃下MoS_2 样品的 X 射线光电子能谱图

Fig.4 XPS spectra of the MoS_2 sample obtained at 240 ℃

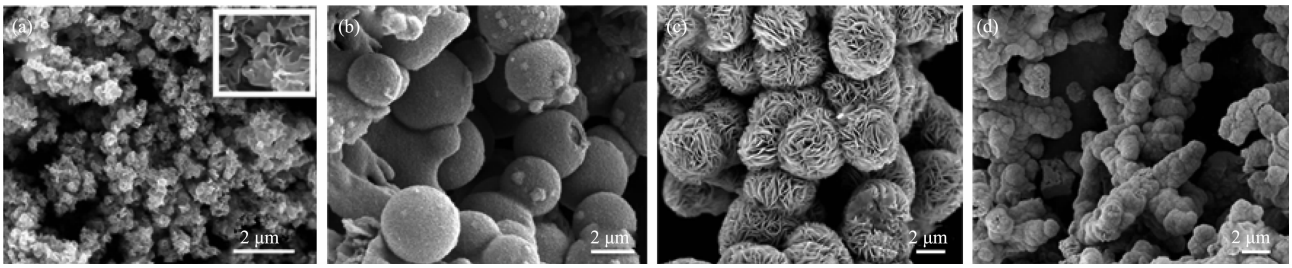

(a) 0; (b) 0.9 mmol; (c) 1.5 mmol; (d) 3.0 mmol

图 5 240 ℃添加不同量Bu_4NBr 制备的 MoS_2 扫描电镜图

Fig.5 SEM images of the obtained MoS_2 structures at 240 ℃ with different amount of Bu_4NBr

2.4 Possible formation mechanism

Ye et al[24] proposed a general method to obtain MoS_2 hierarchical hollow cages. They proved that the Mo oxo anion and tetrabutylammonium cation could

form an intermediate as the template in the formation of MoS_2 hollow cages. Recently, Lis group [25] synthesized MoS_2 microspheres using MoO_3 microbelts as the precursor and Bu_4NBr as the additive by a hydrothermal method. They proposed a possible growth mechanism for the hollow structure. Similarly, based on our experimental results, we believe that it is the Bu_4NBr templating mechanism that should be responsible for the formation of MoS_2 as illustrated in Fig.7. The Bu_4NBr consisting of Bu_4N^+ cation could form many vesicles in the water phase at appropriate concentration. The sulfurization reagent KSCN can easily decompose and form H_2S in acid solution[26]. The surfactant cation and metal oxo anion can co-organize to form periodic surfactant/inorganic composite materials[27]. The Na_2MoO_4 precursor (in the form of MoO_4^{2-} ions) can absorb on the surface of the Bu_4NBr vesicles by the electrostatic interaction. As a result, the hollow spheres are formed during the hydrothermal reaction between MoO_4^{2-} and S^{2-}(Fig.7). The possible reaction route may be expressed as follows:

$$KSCN+2H_2O+HCl \rightarrow NH_3+H_2S+CO_2+NaCl$$

$$4Na_2MoO_4+9H_2S \rightarrow 4MoS_2+Na_2SO_4+6NaOH+6H_2O$$

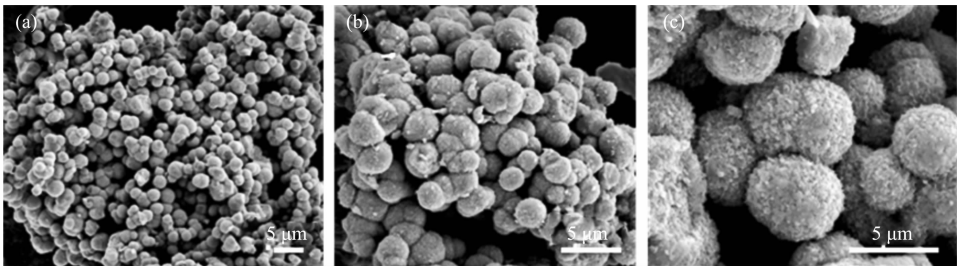

(a) 16 h; (b) 24 h; (c) 48 h

图 6　240 ℃下添加 0.9 mmol Bu_4NBr 在不同反应时间制备的 MoS_2 扫描电镜图

Fig.6　SEM images of MoS_2 nanostructures obtained at 240 ℃ with 0.9 mmol Bu_4NBr at different times

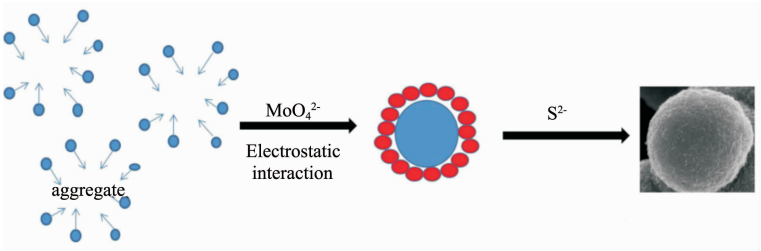

图 7　MoS_2 中空微球形成机理图

Fig.7　Illustration of the formation mechanism of the microspheres MoS_2 structure

2.5 Photocatalytic performance

As shown in Fig.8a, the intensity of the maximum absorption for rhodamine B solution gradually decreases with the increasing of reaction time. One should note that the λ_{max} at 554 nm does not change throughout the reaction process, implying that the ring-open reaction of benzene is predominant in the degradation process[28]. When the reaction time reaches to 45 min, the solution is almost transparent and no fluorescence is shown under ultraviolet light. The calculated degradation rate at 45, 60, 75, and 90 min is 98.5%, 99.2%, 99.4% and 99.6%, respectively, which means that RhB is almost disappeared in the solution after 45 min. In order to clarify the role of the hollow MoS_2 microspheres in these measurements, a control experiment is performed. As shown in Fig. 8b, the degradation rate does not show any changes even at the time of 90 min (1.2%) in the absence of MoS_2. The result indicates that MoS_2 plays an important role in this reaction system. According to the previous work [29], we suggest that the degradation process can be described as follow:

$$MoS_2+H_2O+h\nu \rightarrow Mos_2+\cdot OH+H+\rightarrow$$

$$\cdot OH+RhB \rightarrow CO_2+H_2O$$

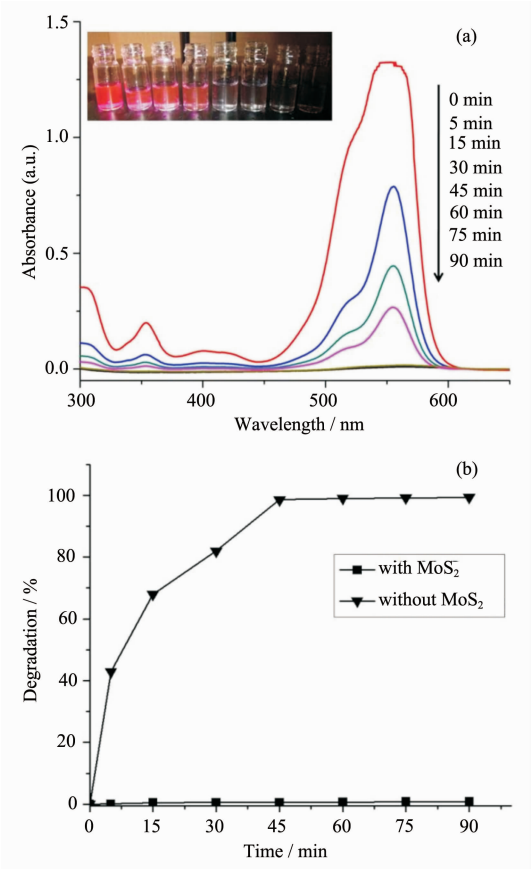

图 8 (a) MoS_2 降解罗丹明 B 的紫外可见吸收光谱图; (b)不同时间下罗丹明 B 的降解率

Fig.8 (a) Absorption spectra (inset: fluorescence image); (b) Degradation rate of RhB at different reaction times

3 Conclusions

MoS_2 hollow microspheres with the diameter of several micrometers were synthesized via a facile hydrothermal route by adding tetrabutylammonium bromide as an additive. FESEM and TEM images show that the size of MoS_2 is 2~5 μm and the spheres are hollow. Higher crystallinity of MoS_2 can be obtained at higher temperature. The effect of the dosage of Bu_4NBr was studied on the growth process of hollow microspheres and the morphology of MoS_2. With the increase in the concentration of Bu_4NBr, the morphology of MoS_2 changes from microspheres, via ball-flowers, to irregular packing. The as-synthesized microstructure exhibits good photocatalytic performance for rhodamine B (RhB) as the target under visible light irradiation. The degradation rate of rhodamine B can be 90%. In addition, the catalytic activity is probably influenced by the morphology of MoS_2, the amount of the MoS_2, the pH value, and the degradation temperature. Further investigations are in progress.

Acknowledgments: This work was supported financially by the National Natural Science Foundation of China (No. 51073059 and No. 91023002), State Key Development Program for Basic Research of China (No. 2009CB930604) and Cooperation Project in Industry, Education and Research of Guangdong Province and Ministry of Education of China (No. 2010B090400123).

References:

[1] Somoano R B, Rembaum A. *Phys. Rev. Lett.*, **1971**,**27**:402-404

[2] Zheng D N, Ramsbottom H D, Hampshire D P. *Phys. Rev. B*, **1995**,**52**:12931-12938

[3] Burlet P, Flouquet J, Genicon J L, et al. *Physica B*, **1995**, **215**:127-133

[4] Peng Z A, Peng X G. *J. Am. Chem. Soc.*, **2001**,**123**:183-184

[5] Rapoport L, Feldman Y, Homyonfer M, et al. *Nature*, **1997**,**387**:791-793

[6] Chen J, Kuriyama N, Yuan H T, et al. *J. Am. Chem. Soc.*, **2001**,**123**:11813-11814

[7] Li Y B, Bando Y, Goldberg D. *Appl. Phys. Lett.*, **2003**,**82**: 1962-1964

[8] Du G D, Guo Z P, Wang S Q, et al. *Chem. Commum.*, **2010**, **46**:1106-1108

[9] Afanasiev P, Bezverkhy I. *J. Phys. Chem. B*, **2003**,**107**:2678-2683

[10]Nath M, Govindaraj A, Rao C N R. *Adv. Mater.*, **2001**,**13**: 283-284

[11]Lin H T, Chen X Y, Li H L, et al. *Mater. Lett.*, **2010**,**64**: 1748-1750

[12]Li W J, Shi E M, Ko J M, et al. *J. Cryst. Growth*, **2003**,**250**: 418-422

[13]Tian Y M, Zhao X, Shen L C, et al. *Mater. Lett.*, **2006**,**60**: 527-529

[14]Wei R H, Yang H B, Du K, et al. *Mater. Chem. Phys.*, **2008**,**108**:188-192

[15]PEI Xiao-Ke(裴小科), LIN Bi-Zhou(林碧洲), ZHANG Jin-Fei(张进飞), et al. *Chinese J. Inorg. Chem.* (*Wuji Huaxue Xuebao*), **2005**,**21**(3):357-362

[16]Ye L, Guo L, Yang Y, et al. *Chem. Mater.*, **2007**,**19**:6331-6337

[17]Ma L, Xu L M, Xu X Y, et al. *Chem. Mater. Lett.*, **2009**,**63**:

2022-2024

[18]Ma L, Chen W X, Li H, et al. *Mater. Chem. Phys*., **2009**, **116**:400-405

[19]Huang W Z, Xu Z D, Liu R, et al. *Mater. Res. Bull*., **2008**, **43**:2799-2808

[20]Luo H, Xu C, Zou D B, et al. *Mater. Lett.*, **2008**,**62**:3558-3560

[21]Wu Z Z, Wang D Z, Sun A K. *J. Mater. Sci.*, **2010**,**45**:182-187

[22]Joensen P, Frindt R F, Morrison S R. *Mater. Res. Bull.*, **1986**,**21**:457-461

[23]Tian Y, He Y, Zhu Y F. *Mater. Chem. Phys*., **2004**,**87**:87-90

[24]Ye L, Guo W, Yang Y, et al. *Chem. Mater.*, **2007**,**19**:6331-6337

[25]Li G, Li C, Tang H, et al. *J. Alloys Compd.*, **2010**,**501**:275-281

[26]Li X L, Li Y D. *J. Phys. Chem. B*, **2004**,**108**:13894-13900

[27]Huo Q, Margolese D I, Ciesla U, et al. *Nature*, **2004**,**368**:317-321

[28]Wu T X, Liu G M, *Zhao J C. J. Phys. Chem. B*, **1998**,**102**:5845-5851

[29]Hu K H, Hu X G, Xu Y F, et al. *Reac. Kinet. Mech. Cat.*, **2010**,**100**:153-163